

## RESIDUAL GAS FLUORESCENCE FOR PROFILE MEASUREMENTS AT THE GSI UNILAC

A. Bank, P. Forck, GSI, Darmstadt, Germany, email: p.forck@gsi.de

### Abstract

The high beam currents, delivered at the LINAC at GSI (UNILAC) can destroy intercepting diagnostics within one macro pulse. As an alternative for a non-destructive profile measurement the method for residual-gas-fluorescence is investigated. The fluorescence light emitted by the  $N_2$  molecules of the residual gas at the blue wavelength range can be monitored with a modern CCD camera. The images are transferred via digital bus and after analysis of the images with a modern software the profiles are generated. Due to the short beam pulses the light intensities emitted by the residual gas are low and require a high amplification which is realized with an image intensifier with double MCP, connected with a fiber taper to the CCD-chip. The design and measurements are discussed.

### Residual Gas Fluorescence

The profile of an ion beam can be determined by observing the fluorescence emitted by the residual gas molecules using a CCD camera. This method was previously applied e.g. at cw proton LINAC at Los Alamos [1] and the CERN SPS synchrotron [2]. The GSI UNILAC is a pulsed heavy ion LINAC with macro pulse lengths of several 100  $\mu$ s and is e.g. used to fill the preceding synchrotron. The beam profile should be monitored within one macro pulse, therefore the use of a long integration time for an improved signal-to-noise ratio is impossible. Because of that short integration time and the pressure of the residual gas (typically:  $10^{-7}$  –  $10^{-8}$  mbar) the emitted light has to be amplified drastically, in this case by using a double MCP image intensifier.

Due to the large energy release in intersecting material (maximum of 1 MW beam power) at high current operation (up to 20 mA beam current) the traditional determination of transverse beam profile by using secondary emission grids (SEM-grids) can not be applied. To prevent melting, the macro pulse length has to be shorted. A non-intersecting residual gas monitor can be installed or the fluorescence of the residual gas can be used to detect the profiles in case of a full pulse length. The latter has the advantage that no mechanical parts have to be installed in the vacuum pipe, leading to a compact and cost-efficient design. In addition the spatial resolution of a SEM-grid is limited by the wire-spacing of about 1 mm. Using the fluorescence method up to 0.1 mm can be achieved. Another advantage is the compact commercial 'data acquisition system' incorporated in the CCD camera.

At GSI UNILAC the ions kinetic energy varies from 0.12 up to 15 MeV/u. Depending on ion type and charge

state this is close to the maximum of the electronic stopping power.

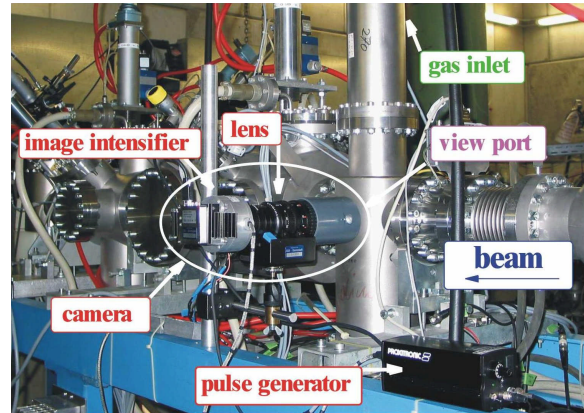


Fig. 1: The installation of the intensified CCD-camera at the target location

The residual gas at the UNILAC contains mainly Nitrogen which has a large cross section for the excitation into the ionized  $N_2^+$  molecular state, as measured in [3] by 200 keV proton collisions and at several GeV in [4]. The fluorescence light is emitted in the wave length range of 300 to 500 nm. A scaling proportional to the electronic stopping power of the beam ions is expected.

### Components

**Vacuum Chamber:** The beam is viewed through a Suprasil window (wavelength transmission between 20 nm and 2  $\mu$ m) mounted on a  $\varnothing$  35 mm flange. To suppress reflections, the tube is blackened by a vacuum suitable graphite lacquer (graphite grains solved in isopropanol).

**Zoom lens:** A remote controlled c-mount zoom lens (Fujinon D14x7.5A-R11/12) with 7.5 – 105 mm focal length and a macro setting is installed. A short distance between the beam and the lens increases the yield of captured photons, but reduces the relative depths of focus. A small focal length increases the depth of focus (i.e. with the same relative iris setting a larger depth can be imaged) but reduces the spatial resolution. A suitable setting was found with a focal length of 15 mm, a distance between lens and center of beampipe of 39 cm resulting in an minimum F-number of 2 (~55 mm depth of focus needed) and an observation length of ~5 cm.

**Image intensifier:** The installed  $\varnothing$ 25 mm image intensifier has a double (chevron) MCP setting with a maximum gain of  $\sim 10^6$ . The captured photons are converted to electrons by a photo-cathode made of S20 UV-enhanced [5], having a quantum efficiency of 25-30

% at the interesting wavelength interval and a low dark current ( $\sim 500$  electrons /  $s \cdot cm^2$ ). The voltage between the photo-cathode and the first MCP can be switched from transfer mode to a blocking mode within 100 ns, enabling an observation only during the beam delivery. This also gives the possibility to observe segments of the macro pulse (see Fig.6). On the P46 phosphor screen spots from single photons are visible. Due to the decay time of the phosphor of  $\sim 300$  ns (90 to 10 %) fast changes of the beam parameters can be resolved. The resolution of  $\sim 0,1$  mm on the MCP surface is sufficient for this application.

**Taper coupling:** To transmit the light from the image intensifier to the CCD a minifying taper coupling is used as shown in Fig.2. This taper is made of bundled glassfibers with shrinking diameter and a minification of 8/25 (ratio of CCD / MCP diameter). About 7 % of the light emitted in the half hemisphere is guided to the CCD which is approximately 5 times of the transmission using a relay optic.

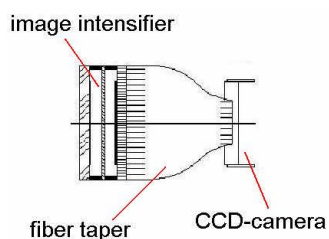


Fig.2: Image intensifier coupled to CCD by reducing taper

**CCD camera:** A 8 bit Basler 302fs CCD camera with a maximum of 28 frames per second at 782 x 582 pixels was chosen. The CCD signals are directly digital-converted at the camera head and transferred using Firewire IEEE1394 [6] protocol. Compared to an analog video link, no degradation of the signal due to long cables occurs. At the moment the Firewire bus standard allows a maximum data rate of 400 Mb/s which equals to 100 frames per second at VGA resolution. The variable bus architecture with up to 63 nodes is well suited for the distributed diagnostic installations in the various beam lines. The maximum cable length for electrical transmission is 20 m. For the long distances between the diagnostics and the control room fiber optic cables driven by opto-couplers (NEC or Newnex Technology) are used.

**Data analysis:** After translation from optical to electrical signal, the data is transferred to a Windows PC via a cheap standard PCI interface. The software to analyse the data is written in Labview. It also allows to control the various camera functions, e.g. exposure time, electronic gain, trigger. The Firewire driver from the commercial package IMAQ is used to acquire the images and control the camera and the IMAQ Vision package for the image processing.

### Test measurements

For the test measurements medium and high current  $Ar^{10+}$  and  $U^{28+}$  beams with energies of 4.7, 5.8 and 11.4 MeV/u are used. Typical currents were 0.5 to 2 mA

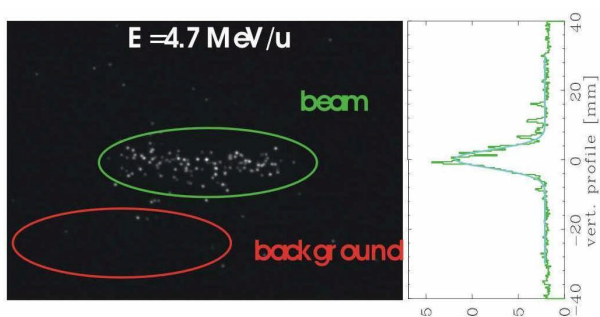


Fig.3: Image of a 200  $\mu s$   $U^{28+}$  beam with  $I=700\mu A$  recorded at the GSI LINAC with a vacuum pressure of about  $10^{-5}$  mbar. The two dimensional image from the intensifier (left) and the projection for the vertical beam profile (right) is displayed.

and 200  $\mu s$  macro pulse length. This corresponds to  $\sim 10^8 \dots 10^9$  particles per macro pulse passing the viewport. In Fig. 2 an image of a single macro pulse  $U^{28+}$  is displayed. By using a regulated gas valve the pressure could be locally raised up to  $10^{-4}$  mbar. Due to the high amplification of the double MCP, single photon events are visible. Projecting the light spots along the beam axis results in the vertical beam profile. The resolution of 300  $\mu m$ /pixel is sufficient for these parameters. For images of less signal strength the data can be binned to improve the signal-to-noise ratio. Due to the statistical nature of the signal generation, the data quality can also be enhanced by data binning of the individual projections or by summing up several images.

The measurements show a low background, especially after blackening of the vacuum chamber. The uniformly distributed dots outside of the beam path seen in Fig.2 are caused by  $\gamma$ - or x-rays hitting the photo cathode generated by nuclear- or atomic inner shell excitations probably at the beam dump located 2 m apart. Their contribution is independent of the optical setting, and even visible if the iris is totally closed. The noise level increases occasionally for some beam settings, this seems to happen while the beam is hitting the aperture at a location near the image intensifier. Even in such case, the images can still be evaluated. Due to the statistical background distribution over the whole image and after projection, the noise level can be subtracted from the data. A assumed relation of the noise level and the beam energy could not be confirmed during the latest tests where a shielding was used to protect the image intensifier from the radiation.

The fluorescence data has been compared with the data of a residual gas monitor located 1m downstream in the beam line. As it can easily be seen in Fig.4 the correspondence is quiet well. In this beam setting the resolution of the fluorescence profile is particularly suitable whereas the residual gas monitor reaches it's border of resolution where only 5 to 7 points are distributed over the whole peak.

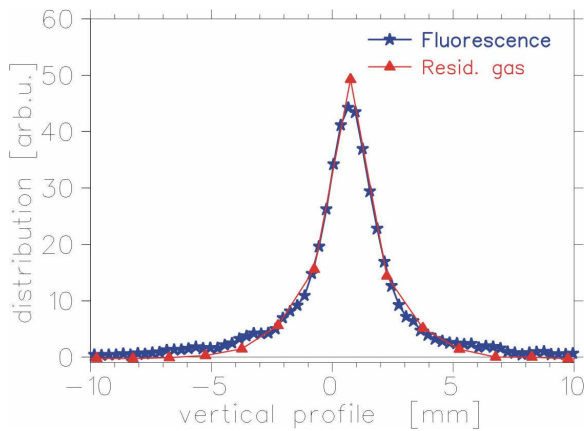


Fig.4: Comparison of the fluorescence profile with the data of a residual gas monitor measured at 11.4 MeV/u. The curves are normalized to the same integral.

A crucial point for the operation of the fluorescence monitor is a proper alignment of the optics. The depth of sharpness has to be defined well by choosing a proper focal length, object distance and iris [7]. A compromise between resolution and signal strength has to be found. It is advantageous to choose a moderate object distance, ~40 cm in our case. The loss of signal and resolution due to the larger distance to the beam is reobtained by the possibility of choosing a larger focal length and iris due to comparable larger depth of focus at that distance. In most cases the optical quality of a lens with small focal length is lower. An array of LED's opposite to the camera is used to match the depth of sharpness with the center of the beam pipe. It is also used as an on-line calibration for the reproduction scale.

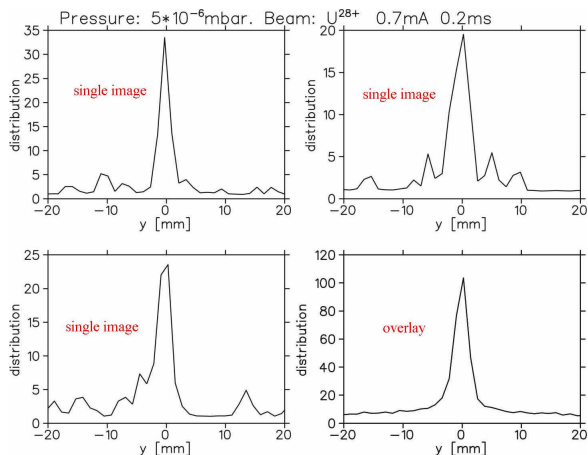


Fig.5: Three vertical projections of images of a single macro pulse and one projection (lower right corner) of an overlay of 32 images. All are made at  $5 \cdot 10^{-6}$  mbar.

The lowest usable residual gas pressure for an optical setting (distance to beam center ~40 cm, focal length 15 mm, F-number 2.8) of the measurements with  $700 \mu\text{A } U^{28+}$  and  $200 \mu\text{s}$  pulse length was found at  $5 \cdot 10^{-6}$  mbar. In Fig.5 3 projections of images of a single macro pulse as well as a projection of 32 consecutive images are shown. The averaging of

images of several macro pulses gives the possibility for further improvement of the signal-to-noise ratio. An advanced application for the residual fluorescence measurement is the determination of the pulse width variation as shown in Fig.6. The fast switching of the voltage between the photocathode and the MCP can be used to restrict the exposure time. For a case of Fig. 6 one image of  $40 \mu\text{s}$  exposure time is recorded and the measurement is repeated with 8 different trigger delays. This type of measurement is not possible with an intersecting SEM-grid due to the risk of wire melting by the large beam power.

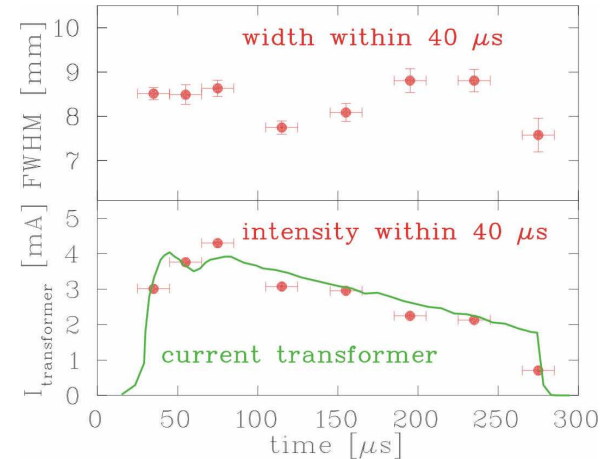


Fig.6: Measurement of the width structure of the macro pulse. In the lower graph the normalized image intensity to the measured beam current.

## Conclusion

The described non-intersecting method for profile measurements can be applied for ion beams of high current at a pulsed LINAC. For a signal enhancement at lower currents, a moderate pressure bump can be applied easily. A direct image of the beam is generated without any installations inside the vacuum pipe. A resolution of up to 0.1 mm can be reached. More advanced detection schemes, e.g. like observation of a possible beam movement during one macro-pulse can be applied by using a short exposure time.

## References

- [1] D.P.Sandoval et al., 5<sup>th</sup> beam Instrum. Workshop, Santa Fe, AIP Conf. Proc. 319, p. 273 (1993).
- [2] G.Burtin et al., Proc. 6<sup>th</sup> Euro. Part. Acc. Conf. EPAC, Vienna, p. 256 (2000).
- [3] R.H.Hughes et al., Phys. Rev. 123, 2048 (1961).
- [4] M.A.Plum et al.Nucl. Instr. And Meth. In Phys. Research A 492 p.74-90 (2002).
- [5] www.proxitronic.de
- [6] D. Anderson, FireWire architecture: 1394a www.mindsharing.com, Addison-Wesley (1999).
- [7] P.Forck, A.Bank, Euro. Part. Acc. Conf. EPAC Paris, p.1885 (2002).